Research Journal of Applied Sciences, Engineering and Technology 4(17): 3108-3118, 2012
ISSN: 2040-7467

Submitted: March 12, 2012 Accepted: April 03, 2012 Published: September 01, 2012

Image Denoising of Wavelet based Compressed Images Corrupted by Additive White Gaussian Noise

[1]Shyam Lal and [2]Mahesh Chandra
[1]ECE Department, Moradabad Institute of Technology, Moradabad (UP), India
[2]ECE Department, Birla Institute of Technology, Mesra, Ranchi (JH), India

Abstract: In this study an efficient algorithm is proposed for removal of additive white Gaussian noise from compressed natural images in wavelet based domain. First, the natural image is compressed by discrete wavelet transform and then proposed hybrid filter is applied for image denoising of compressed images corrupted by Additive White Gaussian Noise (AWGN). The proposed hybrid filter (HMCD) is combination of non-linear fourth order partial differential equation and bivariate shrinkage function. The proposed hybrid filter provides better results in term of noise suppression with keeping minimum edge blurring as compared to other existing image denoising techniques for wavelet based compressed images. Simulation and experimental results on benchmark test images demonstrate that the proposed hybrid filter attains competitive image denoising performances as compared with other state-of-the-art image denoising algorithms. It is more effective particularly for the highly corrupted images in wavelet based compressed domain.

Keywords: Bivariate shrinkage function, fourth order PDE, hybrid filter, image denoising, natural images

INTRODUCTION

Now-a-days an image is synonymous to digital image and is very much essential for daily life applications such as satellite television, medical imaging (i.e., magnetic resonance imaging, ultrasound imaging, x-ray imaging), computer tomography etc. It is also essential for the researches in the areas of science and technology such as geographical information systems and astronomy. The digital images collected by different type of sensors are generally contaminated by different types of noises. Noises may be generated due to imperfect instruments used in image processing, during data acquisition process and interference, all of which can degrade the quality of images. Furthermore, noises can be introduced during data transmission and compression. The compressed domain processing of image is very good for web and internet application because they provides low storage capacity needed and better performances in information transmission through internet. The compressed domain image processing algorithms are encoded in JPEG image domain, which results a powerful computational because there is no need to decompress or recompress the whole image prior to processing or after processing and it computes less data (after quantization many of the DCT coefficients are zero). In case of web application more than 95% of images are in JPEG compressed format but wavelet based compressed domain further increase the performances for transmission of information. The advantages of using 2D discrete wavelet transform are faster, linear in its operation, invertible and orthogonal. Due to this reconstruction is easier. Due to variable window size, they are capable of providing the time and frequency information simultaneously. Compressed image is contaminated by additive white Gaussian noise during transmission through communication channel. Therefore it is important to remove additive white Gaussian noise from the image before some subsequent processing.

Image denoising is very essential to improve the quality of image. During last one decade various image denoising schemes have been proposed by various researchers for the improvement of quality of image. The image denoising schemes such as smoothing filters and frequency domain denoising methods (Gonzalez and Woods, 2002), wavelet based methods (Chang *et al*., 2000; Chen *et al.*, 2005; Donoho, 1995; Coifman and Donoho, 1995; Mıhcak *et al*., 1999; Chang *et al*., 2000; Pizurica *et al.*, 2002; Hou, 2003), curvelet based methods (Starck *et al.*, 2002), ridgelet based methods (Chen and Kegl, 2006), sparse representation method (Elad and Aharon, 2006), K-SVD methods (Aharon *et al*., 2006), shape-adaptive transform (Foi *et al*., 2007), bilateral filtering (Tomasi and Manduchi, 1998; Barash, 2002), non-local mean based methods (Buades *et al.*, 2005; Kervrann and Boulanger, 2006), non local collaborative filtering (Dabov *et al.*, 2007), BiShrink (Sendur and Selesnick, 2002), SURE-LET (Luisier *et al.*, 2007), BlockShrink (Dengwen and Shen, 2008),

Corresponding Author: Shyam Lal, ECE Department, Moradabad Institute of Technology, Moradabad (UP), India

NeighShrink SURE (Dengwen and Cheng, 2008), LPG-PCA (Zhang *et al.*, 2010), NLM-SAP (Deledalle *et al.*, 2011) and non-linear fourth order partial differential equation (You and Kaveh, 2000; Lysaker *et al.*, 2003) are some of the major methods used for AWGN noise removal. Revolution on modern digital imaging devices and their requirements for wide applications in our daily life increases requirements of efficient denoising algorithm for higher image quality.

During last decade, wavelet transform based algorithm is attracted very much because of effective removal of noise from digital images (Chang *et al*., 2000; Chen *et al*., 2005; Donoho, 1995; Coifman and Donoho, 1995; Mıhcak *et al.*, 1999; Chang *et al*., 2000; Pizurica *et al.*, 2002; Hou, 2003). The wavelet transform decomposes the input signal into multiple scales, which represent different time-frequency components of the original signal. Denoising is accomplished by transforming back the processed wavelet coefficients into spatial domain. Late development of wavelet transform based image denoising includes curvelet (Starck *et al*., 2002) and ridgelet (Chen and Kegl, 2006) methods for line structure preservation. Although wavelet transform has demonstrated its efficiency in denoising. It uses a fixed wavelet basis (with dilation and translation) to represent the image. For natural images, however there is a rich amount of different local structural patterns, which cannot be well represented by using only one fixed wavelet basis. Therefore, wavelet transform based methods can introduce many visual artifacts in the image denoising output.

In order to overcome the drawback of wavelet transform based denoising algorithm, spatially adaptive Principal Component Analysis (PCA) based denoising scheme is proposed (Muresan and Parks, 2003). In this algorithm locally fitted basis approach is adapted to transform the image. Sparse redundant representation and K-SVD based denoising algorithms are proposed (Elad and Aharon, 2006; Aharon *et al*., 2006) for image denoising. These two methods are used for training a highly over-complete dictionary for improved image denoising performance. Efficient denoising algorithm is proposed for effective image denoising (Foi *et al*., 2007). This algorithm is applied to a shape-adaptive Discrete Cosine Transform (DCT) to the neighborhood, which results very sparse representation of the images and leads to effective denoising. All these methods show better denoising performance than the conventional wavelet transform based image denoising algorithms. Some of the existing image denoising techniques given below have been implemented and their performances have been compared with the proposed algorithm.

BayesShrink (Chen *et al*., 2005): The main objective of this algorithm is to minimize the bayesian risk and hence its name, BayesShrink. Its denoising performance is poor in high density additive white Gaussian noise.

BiShrink (Sendur and Selesnick, 2002): This method is based on new non-gaussian bivariate distributions to model interscale dependencies. A nonlinear bivariate shrinkage function using the Maximum A Posteriori (MAP) estimator is derived. In a second paper, these authors have extended their approach by taking into account the intrascale variability of wavelet coefficients. Its denoising performance is deteriorates in high density additive white gaussian noise.

SURE-LET (Luisier *et al.*, 2007): This method directly parameterizes the denoising process as a sum of elementary nonlinear processes with unknown weights. It need not hypothesize a statistical model for the noiseless image while it minimizes an estimate of the mean squared error between the noiseless image and the denoised one by the Stein's Unbiased Risk Estimate (SURE). Consequently, it computes the unknown weights by solving a linear system of equations.

BlockShrink (Dengwen and Shen, 2008): This method is completely based on data-driven block thresholding approach. The main advantage of this algorithm is easy to implement. It utilizes the pertinence of the neighbor wavelet coefficients by using the block thresholding scheme. It can decide the optimal block size and threshold for every wavelet subband by minimizing SURE.

NeighShrink SURE (Dengwen and Cheng, 2008): This method is an improved over Neigh Shrink, which can determine an optimal threshold and neighbouring window size for every subband by the SURE. Its denoising performance is considerably superior to NeighShrink and outperforms SURE-LET. It is well known that increasing the redundancy of wavelet transforms can significantly improve the denoising performances.

NLM-SAP (Deledalle *et al*., 2011): In this algorithm the main idea is to replace the usual square patches used for comparing pixel neighborhoods with various shapes that can take advantage of the local geometry of the image. This method provides a fast algorithm to compute the Non local Means with arbitrary shapes. After that they consider local combinations of the estimators associated with various shapes by using SURE.

ProbShrink (Pizurica and Philips, 2006): This algorithm is derived by estimation of the probability that a given coefficient contains significant information. They have also assumed that generalized Laplacian prior for the noise free data.

Although the above image denoising techniques give a better performance in terms of AWGN noise removal. But, they still tend to remove useful details from the image or retain too much AWGN noise in high density of noise occurrence (i.e., noise variance ranging from 50 to

80). In order to overcome this problem, an efficient algorithm is proposed. This algorithm is used for removal of high density additive white Gaussian noise in wavelet based compressed domain. The proposed algorithm provides better noise suppression with keeping minimum edge blurring as compared to other image denoising techniques for highly corrupted natural images in wavelet based compressed domain. The proposed algorithm is used for next generation wireless communication and also suitable for web and internet application.

PROPOSED ALGORITHM

This section start from describing the image compression using 2D discrete wavelet transform and then hybrid filter is proposed for image denoising of wavelet based compressed images. The proposed hybrid filter is applied for image denoising of compressed images corrupted by Additive White Gaussian Noise (AWGN). The proposed hybrid filter works in two phase, in first phase the noisy compressed images is processed by non-linear fourth order PDE and in second phase bivariate shrinkage function based image denoising algorithm is used to further process the output of non-linear fourth order PDE. The scheme of the proposed hybrid filter is shown in Fig. 1.

The noisy image is describes as follows:

$$f(i, j) = c(i, j) + n(i, j) \quad (1)$$

where, c (i, j) is compress image n (i, j) is AWGN noise.

Image compression using discrete wavelet transforms: The main idea behind this method is that it performs image compression very efficiently and gives higher compression ratio and better image qualities as compared to other compression techniques (Chang *et al*., 2000).

The following implementation steps have been made for the image compression using discrete wavelet transform, which is based on 2-D-wavelet:

- Read original image.
- Decomposition of images using wavelets for the level N.
- Selecting and assigning a wavelet for compression.

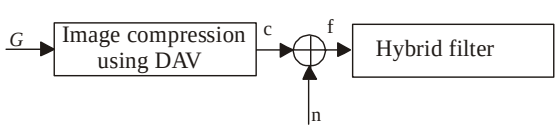

Fig. 1: The block diagram of proposed model

- Generating threshold coefficients.
- Performing the image compression using wavelets.
- Computing and displaying the results such as compressed image, memory size requirements, Compression ratio, PSNR & FSIM.

Hybrid filter: This section describes proposed Hybrid filter (HMCD) for image denoising of wavelet based compressed images corrupted by additive white Gaussian noise. The proposed hybrid filter is combination of non-linear fourth order partial differential equation and bivariate shrinkage function. The reason behind using non-linear fourth order partial differential equation is that it is comparatively a very good approach for effective image denoising. During last decade, a number of non-linear fourth order partial differential equations have been proposed for image denoising (Rajan *et al*., 2008). Although discrete implementation of these methods produces impressive results because of various mathematical properties. The discrete form of non-linear fourth order PDE described in Eq. (2) is as follows:

$$u_{i,j}^{n+1} = u_{i,j}^{n} - \Delta t \nabla^2 g_{i,j}^{n} \quad (2)$$

$$\nabla^2 g_{i,j}^{n} = \frac{g_{i+1,j}^{n} + g_{i-1,j}^{n} + g_{i,j+1}^{n} + g_{ij-1}^{n} - 4g_{i,j}^{n}}{h^2} \quad (3)$$

$$g_{i,j}^{n} = g(\nabla^2 u_{i,j}^{n}) \quad (4)$$

$$\nabla^2 u_{i,j}^{n} = \frac{u_{i+1,j}^{n} + u_{i-1,j}^{n} + u_{i,j+1}^{n} + u_{i,j-1}^{n} - 4u_{i,j}^{n}}{h^2} \quad (5)$$

Δt is the time step size and h is the space grid size. The fourth order diffusion (Greer, 2003) is derived from a variational formulation which is similar to the second order total variation method (Rudin *et al*., 1992). It is observed in Greer (2003) that the equation is linearly ill posed in the regions of high curvature. In second stage bivariate shrinkage function based local adaptive algorithm is used to further process the output of first stage (Sendur and Selesnick, 2002). This algorithm is combined with Eq. (2) to remove high density additive white Gaussian noise in wavelet based compressed domain. The proposed hybrid filter is defined as follows:

$$u_{i,j}^{n+1} = LAA(u_{i,j}^{n} - \Delta^2 g_{i,j}^{n}) \quad (6)$$

where, LAA is local adaptive algorithm based on bivariate shrinkage funct0ion.

The working of a local adaptive algorithm based on bivariate shrinkage function is as follows: The denoising

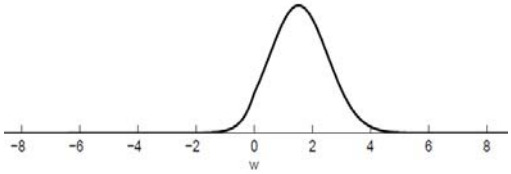

Fig. 2: The MAP estimate w is the point where the pdf has its peak

of image corrupted by additive independent white Gaussian noise with variance σ^2_n will be considered. Let w_{2k} represent the parent of w_{1k} (w_{2k} is the wavelet coefficient at the same position as the k^{th} wavelet coefficient w_{1k}, but at the next coarser scale).We formulate the problem in wavelet domain as $y_{1k} = w_{1k}+n_{1k}$ and $y_{2k}=w_{2k}+n_{2k}$ to take into account the statistical dependencies between a coefficient and its parent. y_{1k} and y_{2k} are noisy observations of w_{1k} and w_{2k} and , n_{1k} and n_{2k} are noise samples (Rajan *et al.*,2008; Rao *et al*., 2009; Selesnick, 2009). It can be written as:

$$y_k = w_k+n_k,\ k = 1\ldots.\ \text{no.of wavlet cofficients} \quad (7)$$

where, $w_k = (w_{1k}, w_{2k})$, $y_k = (y_{1k}, y_{2k})$ and $n_k = (n_{1k}, n_{2k})$. From this point, the coefficient index *k* will be omitted from the equations in order to improve the readability of the equations. The standard Maximum A Posteriori (MAP) estimator for w given the corrupted observation y is:

$$\hat{w}(y) = \arg\max_{w} \quad p_{w|y}(w|y) \quad (8)$$

where, "arg max" is the value of the argument where the function has its maximum. The probability density function (pdf) $p_{w|y}(w|y)$ is the distribution of w given a specific value y and it is shown in Fig. 2.

To find the value of w where $p_{w|y}(w|y)$ has its peak, note that:

$$p_{w|y}(w|y) = \frac{p_{w,y}(w,y)}{p_y(y)} \quad (9)$$

and

$$p_{y|w}(y|w) = \frac{p_{w,y}(w,y)}{p_w(w)} \quad (10)$$

So rearranging terms we get:

$$p_{w|y}(w|y) = \frac{p_{y|w}(y|w)\,p_w(w)}{p_y(y)} \quad (11)$$

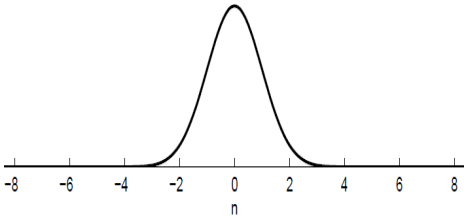

Fig. 3: The pdf, p_n (n), of a zero-mean Gaussian random variable

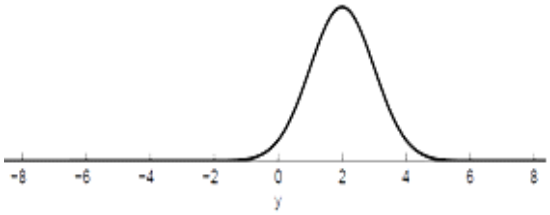

Fig. 4: The pdf, p_n (y – 2), of a Gaussian random variable with mean 2

Equation (11) is Bayes rules. Therefore, one gets:

$$\hat{w} = \arg\max_{w}\left[\frac{p_{y|w}(y|w)\,p_w(w)}{p_y(y)}\right] \quad (12)$$

In Eq. (12) the term $p_y(y)$ does not depend on w, so the value of w that maximizes right-hand side is not influenced by the denominator. Therefore the MAP estimate of w is given by:

$$\hat{w} = \arg\max_{w}\left\{p_{y|w}(y|w).\,p_w(w)\right\} \quad (13)$$

The conditional pdf $p_{y|w}(y|w)$ can be found by noting that given w, we have that y = w+n is the sum of w and a zero-mean Gaussian random variable. For example, if n is a zero-mean Gaussian random variable, then its pdf will be centered around 0 and it is shown in Fig. 3 and 2 + n is a Gaussian random variable with mean 2 and the pdf will be centered around 2 and it is shown in Fig. 4.

Similarly, if w is known, then w + n is a Gaussian random variable with mean w and the pdf will be centered around w. Therefore, y = w+n is Gaussian with mean w. That is: $p_{y|w}(y|w) = p_n(y-w)$

Therefore $p_{y|w}(y|w) = p_n(y-w)$ and the estimate can be written as:

$$\hat{w}(y) = \arg\max_{w}\left[p_n(y|w).\,p_w(w)\right] \quad (14)$$

Non-Gaussian bivariate probability distribution function is proposed to model the statistics of wavelet coefficients of natural images (Sendur and Selesnick, 2002). The model captures the dependence between a wavelet coefficient and its parent. Using Bayesian estimation theory a simple non-linear shrinkage function for wavelet denoising is derived from this model, which generalizes the soft thresholding approach of Donoho and Johnstone (1994). The shrinkage function, which depends on both the coefficient and its parent, yields improved results for wavelet-based image denoising (Sendur and Selesnick, 2002; Rajan *et al.*, 2008; Selesnick, 2009; Rao *et al.*, 2009). The non-Gaussian bivariate probability distribution function for the coefficient and its parent is given as:

$$p_w(w) = \frac{3}{2\pi\sigma^2}.\exp\left(-\frac{\sqrt{3}}{\sigma}\sqrt{\left(w_1^2 + w_2^2\right)}\right) \quad (15)$$

The marginal variance σ^2 is also dependent on the coefficient index k . Using (15) with (14), the MAP estimator of w_1 is derived to be:

$$\hat{w} = \frac{\left[\sqrt{\left(y_1^2 + y_2^2\right)} - \frac{\sqrt{3}\sigma_n^2}{\sigma}\right]}{\sqrt{\left(y_1^2 + y_2^2\right)}}.y_1 \quad (16)$$

For this bivariate shrinkage function, the smaller the parent value the greater the shrinkage. This is consistent with other models, but here it is derived using a Bayesian estimation approach.

This estimator requires the prior knowledge of the noise variance σ^2_n and the marginal variance $\sigma^2$for each wavelet coefficient. In this algorithm, the marginal variance for the k^{th} coefficient will be estimated using neighboring coefficients in the region N(k). Here N(k) is defined as all coefficients within a square-shaped window that is centered at the k^{th} coefficient. In order to estimate the noise variance $\sigma^2_n$from the noisy wavelet coefficients, a robust median estimator is used from the finest scale wavelet coefficients:

$$\hat{\sigma}_n^2 = \frac{median\left(|y_i|\right)}{0.64745}, y_i \in subband\ HH \quad (17)$$

Let us assume we are trying to estimate the marginal variance $\sigma^2$for the k^{th} wavelet coefficient. From above observation model, one gets $\sigma^2_y = \sigma^2+\sigma^2_n$ where, σ^2_y the marginal variance of noisy observations are y_1 and y_2. Since y_1 and y_2 are modeled as zero mean, σ^2_y can be found empirically by:

$$\hat{\sigma}_y^2 = \frac{1}{M}\sum\nolimits_{yi} N(k) y_i^2 \quad (18)$$

where, M is the size of the neighborhood N(k). Then, can σ be estimated as:

$$\hat{\sigma} = \sqrt{\left(\hat{\sigma}_y^2 - \hat{\sigma}_n^2\right)} \quad (19)$$

When non-linear fourth order PDE is applied to compressed images, the areas having small gradients are smoothed and which having large gradients (edges and noise if any) remain undiffused and the blocky effects can be avoided. The gradients generated by noise can be subsequently removed by bivariate shrinkage function based local adaptive image denoising algorithm without affecting the image structure. However if the gradients are generated by edges, the bivariate shrinkage function based local adaptive image denoising algorithm will not affect them. So as iteration continues, the non-linear PDE removes the low level noise and subsequently the bivariate shrinkage function based local adaptive image denoising algorithm removes the high level noise. The proposed hybrid filter preserves image quality much better than the other denoising algorithms in compressed domain.

SIMULATION AND EXPERIMENTAL RESULTS

In order to demonstrates the performance of proposed Hybrid filter (HMCD), the 8-bit image of dimensions Ml×M2 (= 256×256) pixels is used for simulation. The image is corrupted by adding additive white Gaussian noise with noise variance (σ) ranging from 10 to 80. In order to judge the performance of the image denoising techniques Peak Signal to Noise Ratio (PSNR) and Mean Squared Error (MSE) are the automatic choice for the researchers. But a better PSNR does not imply that the visual quality of the image is good. In order to overcome this problem FSIM, A Feature Similarity Index for Image Quality Assessment (Zhang *et al.*, 2011) has been considered in this work as the second parameter for judging the quality of denoised images. The superiority of different image denoising algorithm is demonstrated by conducting two experiments. The image Compression Ratio (CR) defined in Eq. (20) is the metric used to compare the performance of the image compression. Further Peak Signal to Noise Ratio (PSNR) & FSIM index are defined in Eq. (21) and (22) respectively. These are the metrics used to compare the performance of image denoising capability of 4thOrder PDE (You and Kaveh, 2000), BayesShrink (Chen *et al.*, 2005), BiShrink (Sendur and Selesnick, 2002), SURE-LET (Luisier *et al.*, 2007),

Table 1: Comparative performance of image compression using discrete wavelet transform for different images

	Original image		Compressed image					
Image	Size	Memory requirement (in bytes)	Size	Memory requirement (in bytes)	Compression ratio	MSE	PSNR	FSIM
Lena	256x256	72670	256x256	1322	54.97	36.36	32.52	0.95
House	256x256	52124	256x256	1286	40.53	12.64	37.12	0.97
Fruits	256x256	66732	256x256	1306	51.10	17.72	35.65	0.96
Peppers	256x256	67455	256x256	1870	36.07	27.09	33.80	0.96

Table 2: Comparative PSNR (dB) value of different methods in wavelet based compressed domain

		Method image								
		4^{th} order PDE	Byes shrink	Bi shrink	Block shrink	Neigh shrink SURE	Prob shrink	SURE-LET	NLM-SAP	HMCD
Fruits	σ = 10	29.68	33.58	34.31	33.70	34.36	34.59	34.37	34.75	34.67
256X256	σ = 20	28.11	30.05	30.90	30.10	31.01	31.26	30.86	31.48	31.34
	σ = 30	25.34	28.08	28.98	28.05	29.09	29.11	28.85	29.16	29.42
	σ = 40	22.34	26.65	27.64	26.61	27.74	27.65	27.44	27.53	28.04
	σ = 50	19.76	25.53	26.61	25.54	26.75	26.57	26.37	26.29	26.99
	σ = 60	17.67	24.61	25.78	24.67	25.94	25.68	25.52	25.35	26.15
	σ = 70	15.99	23.88	25.06	23.96	25.26	24.96	24.82	24.60	25.43
	σ = 80	14.62	23.25	24.43	23.34	24.64	24.36	24.23	23.98	24.81
House	σ = 10	29.34	33.79	35.10	34.12	35.09	35.34	35.11	36.30	35.58
256X256	σ = 20	27.78	30.18	31.35	30.22	31.48	31.57	31.32	33.10	31.90
	σ = 30	25.09	28.14	29.34	28.15	29.51	29.43	29.24	30.57	29.87
	σ = 40	22.13	26.73	27.97	26.86	28.15	28.05	27.83	28.55	28.49
	σ = 50	19.51	25.71	26.94	25.82	27.05	27.02	26.77	26.94	27.46
	σ = 60	17.38	24.82	26.10	24.91	26.24	26.17	25.94	25.73	26.61
	σ = 70	15.67	24.09	25.40	24.18	25.57	25.48	25.24	24.83	25.90
	σ = 80	14.29	23.38	24.81	23.59	24.96	24.90	24.65	24.13	25.32
Lena	σ = 10	27.15	31.69	33.09	32.34	32.94	33.02	33.01	33.47	33.34
256X256	σ = 20	26.18	28.13	29.15	28.49	29.11	29.32	29.11	29.94	29.41
	σ = 30	24.22	26.29	27.12	26.50	27.10	27.28	27.11	27.99	27.39
	σ = 40	21.78	24.98	25.79	25.19	25.81	25.85	25.80	26.50	26.08
	σ = 50	19.45	24.07	24.79	24.27	24.87	24.90	24.84	25.01	25.18
	σ = 60	17.45	23.37	24.00	23.50	24.11	24.20	24.10	24.23	24.32
	σ = 70	15.80	22.74	23.37	22.86	23.49	23.60	23.49	23.54	23.70
	σ = 80	14.44	22.15	22.83	22.22	22.90	23.02	22.97	22.90	23.18
Peppers	σ = 10	27.95	32.05	33.03	32.38	32.97	33.39	33.32	33.88	33.48
256X256	σ = 20	26.74	28.44	29.03	28.41	29.08	29.66	29.40	30.62	29.53
	σ = 30	24.52	26.28	26.94	26.35	27.05	27.61	27.22	28.67	27.45
	σ = 40	21.88	24.91	25.54	24.96	25.62	26.15	25.70	27.07	26.04
	σ = 50	19.42	23.86	24.47	23.81	24.60	24.98	24.55	24.99	25.12
	σ = 60	17.37	22.70	23.60	22.93	23.73	23.94	23.64	24.22	24.57
	σ = 70	15.70	22.05	22.86	22.06	23.05	23.11	22.92	23.21	23.52
	σ = 80	14.33	21.47	22.23	21.40	22.41	22.45	22.34	22.27	22.69

BlockShrink (Dengwen and Shen, 2008), NeighShrink SURE (Dengwen and Cheng, 2008), ProbShrink (Pizurica and Philips, 2006) and NLM-SAP (Deledalle *et al.*, 2011) with proposed Hybrid filter (HMCD) the image Compression Ratio (CR) is defined as:

CR = Number of bits in Original image /Number of bits in Compressed image (20)

The PSNR between the transformed output image u(i, j) and the original image g(i, j) of dimensions MlxM2 pixels is defined as:

$$PSNR = 10 \times \log_{10}\left(\frac{255^2}{MSE}\right) \quad (21)$$

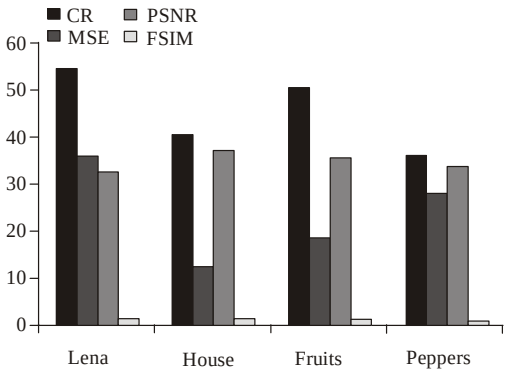

Fig. 5: Image compression performance of different image using DWT

Table 3: Comparative MSE value of different methods in wavelet based compressed domain

		Method image								
		4th order PDE	Byes shrink	Bi shrink	Block shrink	Neigh shrink SURE	Prob shrink	SURE-LET	NLM-SAP	HMCD
Fruits	σ = 10	70.01	28.49	24.08	27.71	23.84	22.59	23.78	21.78	22.21
256X256	σ = 20	100.54	64.22	52.81	63.60	51.49	48.64	53.35	49.26	47.75
	σ = 30	190.14	101.18	82.26	101.78	80.18	79.79	84.74	78.93	74.39
	σ = 40	379.08	140.47	112.04	141.97	109.41	111.59	117.12	114.95	102.03
	σ = 50	687.18	182.04	141.80	181.46	137.40	143.25	149.85	152.61	130.06
	σ = 60	1111.05	224.83	171.98	221.62	165.56	175.63	182.35	189.92	157.96
	σ = 70	1635.82	266.42	202.91	261.26	193.64	207.33	214.17	225.53	186.19
	σ = 80	2242.64	307.98	234.43	301.39	223.61	238.42	245.37	259.78	214.60
House	σ = 10	75.71	27.14	20.09	25.19	20.13	20.02	20.24	20.14	18.00
256X256	σ = 20	108.52	62.40	47.66	61.86	46.22	45.27	48.02	31.84	42.02
	σ = 30	201.48	99.76	75.78	99.55	72.73	74.13	77.48	57.06	67.01
	σ = 40	398.44	138.06	103.74	134.10	99.50	101.95	107.28	90.86	92.04
	σ = 50	727.94	174.71	131.43	170.28	128.20	129.22	136.68	131.52	116.67
	σ = 60	1189.86	214.52	159.63	210.14	154.70	157.10	165.69	173.65	141.89
	σ = 70	1763.90	253.72	187.58	248.57	180.50	184.01	194.43	213.85	166.95
	σ = 80	2423.71	298.59	214.72	284.54	207.61	210.64	222.95	251.40	191.18
Lena	σ = 10	125.20	44.06	31.93	37.98	33.04	32.44	32.52	32.21	30.15
256X256	σ = 20	156.88	100.12	79.05	92.08	79.74	74.84	79.83	75.90	74.52
	σ = 30	245.94	152.80	126.21	145.53	126.85	116.23	126.56	123.38	118.58
	σ = 40	431.67	206.64	171.28	196.95	170.76	157.66	171.02	185.42	160.43
	σ = 50	738.77	254.64	216.02	243.22	211.78	227.40	213.16	201.33	197.21
	σ = 60	1169.71	299.21	258.59	290.55	252.56	256.35	253.16	249.86	240.74
	σ = 70	1711.24	346.39	299.62	336.22	291.20	283.25	291.40	287.67	277.53
	σ = 80	2338.90	396.04	338.65	390.40	333.80	338.91	328.32	333.82	312.79
Peppers	σ = 10	104.31	40.58	32.36	37.60	32.78	30.16	30.29	30.61	29.20
256X256	σ = 20	137.73	93.10	81.24	93.68	80.39	75.35	74.65	76.39	72.54
	σ = 30	229.76	153.30	131.47	150.52	128.31	118.84	123.28	149.34	116.97
	σ = 40	422.01	210.02	181.51	207.55	178.07	187.85	175.11	187.73	161.83
	σ = 50	742.41	267.07	232.46	270.44	225.54	216.66	228.32	209.53	200.02
	σ = 60	1190.55	348.93	283.98	331.00	275.77	262.21	281.15	250.06	227.02
	σ = 70	1750.94	405.77	336.77	404.30	322.51	317.52	331.95	317.79	289.12
	σ = 80	2397.19	463.65	389.21	471.18	373.68	369.73	379.56	385.72	350.01

where, $MSE = \frac{1}{M_1 \times M_2} \sum_{i}^{M_1} \sum_{j}^{M_2} \left[u(i,j) - g(i,j)\right]^2$

The FSIM, A Feature Similarity Index for Image Quality Assessment for gray scale image between original (g) and denoising image (u) is defined as follows:

$$FSIM = \frac{\sum X \in \Omega S_L(X).PC_m(X)}{\sum X \in \Omega PC_m(X)} \quad (22)$$

where, Ω means the whole image spatial domain.

Where, $S_L = SP_C(X).S_G(X)$

$PC_M = \max(PC_1(X), PC_2(X))$

$SP_C(X) = 2PC_1(X).PC_2(X)+T_1/PC^2{}_1(X)+PC^2{}_2(X)+T_1$

$S_G(X) = 2G_1(X).G_2(X)+T_2/G^2{}_1(X)+G^2{}_2(X)+T_2$

$PC_1(X)$-Phase Congruency (PC) of original image

$PC_2(X)$-Phase Congruency (PC) of denoised image

$G_1(X)$-Gradient Magnitude (GM) of original image

$G_2(X)$-Gradient Magnitude (GM) of denoised image

T_1-is a positive constant to increase the stability of S_{PC}

T_2-is a positive constant depending on the dynamic range of GM values

Experiment 1: In this experiment Fruits, House, Lena and Peppers compressed images are corrupted with different noise variance (σ) ranging from 10 to 80. Various state-of-art image denoising techniques such 4th Order PDE (You and Kaveh, 2000), BayesShrink (Chen *et al*., 2005), BiShrink (Sendur and Selesnick, 2002; Sendur and Selesnick, 2002), SURE-LET (Luisier *et al.*, 2007), BlockShrink (Dengwen and Shen, 2008), NeighShrink SURE (Dengwen and Cheng, 2008), ProbShrink (Pizurica and Philips, 2006) and NLM-SAP (Deledalle *et al.*, 2011) are used to compare the image denoising performance capability with proposed Hybrid filter (HMCD) in wavelet based compressed domain.

Table 4: Comparative FSIM value of different methods in wavelet based compressed domain

		Method								
image		4th order PDE	Byes shrink	Bi shrink	Block shrink	Neigh shrink SURE	Prob shrink	SURE-LET	NLM-SAP	HMCD
Fruite	σ = 10	0.89	0.93	0.94	0.93	0.94	0.95	0.94	0.95	0.95
253X256	σ= 20	0.89	0.88	0.90	0.88	0.90	0.91	0.90	0.92	0.92
	σ = 30	0.85	0.85	0.87	0.85	0.87	0.88	0.87	0.88	0.89
	σ = 40	0.77	0.82	0.85	0.82	0.85	0.85	0.85	0.86	0.87
	σ = 50	0.68	0.80	0.83	0.80	0.83	0.83	0.83	0.83	0.85
	σ = 60	0.60	0.78	0.82	0.78	0.82	0.82	0.81	0.82	0.83
	σ = 70	0.54	0.77	0.80	0.77	0.80	0.80	0.80	0.80	0.82
	σ = 80	0.49	0.75	0.79	0.76	0.79	0.79	0.79	0.79	0.81
House	σ = 10	0.86	0.92	0.94	0.92	0.94	0.94	0.94	0.95	0.95
256X256	σ = 20	0.85	0.86	0.89	0.85	0.89	0.89	0.88	0.92	0.91
	σ = 30	0.80	0.82	0.86	0.81	0.86	0.84	0.85	0.89	0.87
	σ = 40	0.72	0.79	0.83	0.78	0.83	0.82	0.82	0.86	0.85
	σ = 50	0.64	0.76	0.81	0.76	0.80	0.79	0.80	0.83	0.83
	σ = 60	0.57	0.74	0.79	0.73	0.79	0.78	0.78	0.80	0.81
	σ = 70	0.51	0.72	0.78	0.71	0.77	0.76	0.76	0.77	0.80
	σ = 80	0.47	0.70	0.77	0.70	0.76	0.75	0.75	0.75	0.79
Lena	σ = 10	0.87	0.93	0.94	0.93	0.94	0.95	0.94	0.95	0.95
256X256	σ = 20	0.87	0.87	0.90	0.87	0.90	0.90	0.89	0.91	0.91
	σ = 30	0.83	0.83	0.86	0.83	0.86	0.87	0.85	0.88	0.88
	σ = 40	0.77	0.80	0.84	0.81	0.83	0.84	0.83	0.86	0.86
	σ = 50	0.69	0.78	0.82	0.79	0.81	0.82	0.81	0.84	0.84
	σ = 60	0.62	0.77	0.81	0.77	0.79	0.80	0.79	0.82	0.82
	σ = 70	0.56	0.75	0.79	0.76	0.78	0.79	0.78	0.80	0.81
	σ = 80	0.51	0.74	0.78	0.74	0.76	0.78	0.76	0.78	0.80
Peppers	σ = 10	0.88	0.93	0.94	0.93	0.94	0.94	0.94	0.95	0.95
256X256	σ = 20	0.87	0.87	0.88	0.87	0.89	0.90	0.89	0.92	0.91
	σ = 30	0.84	0.84	0.85	0.83	0.85	0.87	0.86	0.90	0.87
	σ = 40	0.77	0.81	0.82	0.80	0.82	0.84	0.83	0.88	0.85
	σ = 50	0.69	0.78	0.81	0.78	0.80	0.82	0.81	0.85	0.83
	σ = 60	0.62	0.76	0.79	0.76	0.78	0.80	0.79	0.83	0.81
	σ = 70	0.56	0.74	0.77	0.74	0.76	0.79	0.78	0.81	0.80
	σ = 80	0.51	0.73	0.76	0.72	0.74	0.78	0.77	0.79	0.79

Image compression performance of Fruits, House, Lena and Peppers images using 2D discrete wavelet transform is given in Table 1 and graphical illustration of wavelet based image compression performance of Fruits, House, Lena and Peppers image is shown in Fig. 5. Peak Signal to Noise Ratio (PSNR) and Mean Squared Error (MSE) are obtained of various state-of-art image denoising techniques for Fruits, House, Lena and Peppers images are given in Table 2 and 3. It can be noticed from Table 2 and 3 that the proposed hybrid filter provides better results as compared to others state-of-art image denoising techniques in compressed domain and it is particularly effective for highly corrupted image (i.e., noise variance ranging from 50 to 80).

Experiment 2: In order to perform the superiority of proposed Hybrid filter (HMCD) another experiment is conducted in which to visualize the subjective image enhancement performance in compressed domain, the enhanced Fruits, Lena and Peppers images are compared with various state-of-art image denoising techniques such as 4th Order PDE (You and Kaveh, 2000), BayesShrink (Chen *et al*., 2005), BiShrink (Sendur and Selesnick, 2002; Sendur and Selesnick, 2002), SURE-LET (Luisier *et al*., 2007), BlockShrink (Dengwen and Shen, 2008), NeighShrink SURE (Dengwen and Shen, 2008), ProbShrink (Pizurica and Philips, 2006) and NLM-SAP (Deledalle *et al.*, 2011) are compared with proposed hybrid filter which are shown from Fig. 6, 7 and 8 and Table 4 gives visual image quality measurement index parameter (i.e. FSIM) for all algorithms. It can be noticed from Table 4 that FSIM index of proposed algorithm is superior as compared to various state-of-art image denoising techniques and it is particularly effective for highly corrupted image (i.e., noise variance ranging from 50 to 80).

CONCLUSION

In this study the performance of proposed Hybrid filter (HMCD) has been compared with other existing image denoising techniques in wavelet based compressed domain for image enhancement purpose. The proposed hybrid filter has shown its superiority over other

Fig. 6a: Original image

Fig. 6b: Compressed image

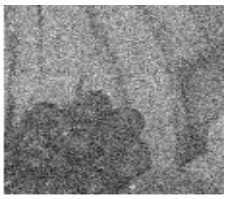

Fig. 6c: Noisy image (σ = 60)

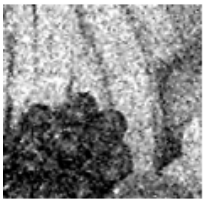

Fig. 6d: Output of 4th order PDE

Fig. 6e: Output of byesshrink

Fig. 6f: Output of bishrink

Fig. 6g: Output of block shrink

Fig. 6h: Output of neighshrink SURE

Fig. 6i: Output of SURE-LET

Fig. 6j: Output of probshrink

Fig. 6k: Output of NLM-SAP

Fig. 6l: Output of HMCD

Fig. 7a: Original image

Fig. 7b: Compressed image

Fig. 7c: Noisy image (σ = 60)

Fig. 7d: Output of 4th order PDE

Fig. 7e: Output of byesshrink

Fig. 7f: Output of bishrink

Fig. 7g: Output of block shrink

Fig.7h: Output of neighshrink SURE

Fig. 7i: Output of SURE-LET

Fig. 7j: Output of probshrink

Fig. 7k: Output of NLM-SAP

Fig. 7l: Output of HMCD

Fig. 8a: Original image

Fig. 8b: Compressed image

Fig. 8c: Noisy image ($\sigma = 60$)

Fig. 8d: Output of 4th order PDE

Fig. 8e: Output of byesshrink

Fig. 8f: Output of bishrink

Fig. 8g: Output of block shrink

Fig. 8h: Output of neighshrink SURE

Fig. 8i: Output of SURE-LET

Fig. 8j: Output of probshrink

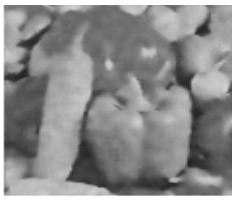

Fig.8k: Output of NLM-SAP

Fig. 8l: Output of HMCD

denoising algorithms for noise removal of compressed natural images corrupted by additive white Gaussian noise. Simulation & experimental results demonstrated that proposed hybrid filter provide better performance in terms of noise removal with minimum edge blurring and better FSIM index as compared to other image denoising techniques in wavelet based compressed domain. Further proposed hybrid filter is suitable for highly corrupted images in wavelet based compressed domain.

REFERENCES

Aharon, M., M. Elad, A. M. Bruckstein, 2006. The K-SVD: An algorithm for designing of overcompletes dictionaries for sparse representation. IEEE Trans. Signal Process., 54(11): 4311-4322.

Buades, A., B. Coll, J.M. Morel, 2005. A review of image denoising algorithms with a new one. Multiscale Model. Simulat., 4(2): 490-530.

Barash, D., 2002. A fundamental relationship between bilateral filtering, adaptive smoothing and the nonlinear diffusion equation. IEEE Trans. Pattern Anal. Mach. Intell., 24(6): 844-847.

Chen, G.Y. and B. Kegl, 2006. Image denoising with complex ridgelets. Pattern Recogn., 40(2): 578-585.

Chen, G.Y., T.D. Bui and A. Krzyzak, 2005. Image denoising with neighbour dependency and customized wavelet and threshold. Pattern Recogn. Lett., 38: 115-124.

Coifman, R.R. and D.L. Donoho, 1995. Translation invariant denoising, wavelets and Statistics. Springer Lect. Notes Statist., 103: 125-150.

Chang, S.G., B. Yu and M. Vetterli, 2000. Adaptive wavelet thresholding for image denoising and compression. IEEE Trans. Image Process., 9(9): 1532-1546.

Chang, S.G., B. Yu, M. Vetterli, 2000. Spatially adaptive wavelet thresholding with context modeling for image denoising. IEEE Trans. Image Process., 9(9): 1522-1531.

Deledalle, A. Charles, D. Vincent and S. Joseph, 2011. Non-local methods with shape-adaptive patches (NLM-SAP). J. Mathemat. Imag. Vision, DOI: 10.1007/ s10851-011-0294-y.

Dabov, K., A. Foi, V. Katkovnik and K. Egiazarian, 2007. Image denoising by sparse 3D transform-domain collaborative filtering. IEEE Trans. Image Process., 16(8): 2080-2095.

Donoho, D.L., 1995. Denoising by soft thresholding. IEEE Trans. Informat. Theor., 41: 613-627.

Donoho, D. L. and Johnstone, I. M. 1994. Ideal spatial adaptation by wavelet shrinkage. Biometrika, 81(3): 425–455.

Dengwen, Z. and X. Shen, 2008. Image Denoising Using Block Thresholding, Congress on Image and Signal Processing (978-0-7695-3119-9/08, IEEE DOI: 10.1109/CISP.2008.131.

Dengwen, Z. and W. Cheng, 2008. Image denoising with an optimal threshold and neighbouring window. Pattern Recogn. Lett., 29: 1694-1697.

Elad, M. and M. Aharon, 2006. Image denoising via sparse and redundant representations over learned dictionaries. IEEE Trans. Image Process., 15(12): 3736-3745.

Foi, A., V. Katkovnik and K. Egiazarian, 2007. Pointwise shape-adaptive DCT for high-quality denoising and deblocking of grayscale and color images. IEEE Trans. Image Process., 16(5): 1395-1411.

Gonzalez, R.C. and R.E. Woods, 2002. Digital Image Processing. 2nd Edn., Prentice Hall, Englewood Cliffs, NJ.

Greer, J.B., 2003. Fourth order diffusion for image processing. Ph.D. Thesis, Department of Mathematics, Duke University.

Hou, Z., 2003. Adaptive singular value decomposition in wavelet domain for image denoising. Pattern Recogn., 36(8): 1747-1763.

Kervrann, C. and J. Boulanger, 2006. Optimal spatial adaptation for patch based image denoising. IEEE Trans. Image Process., 15(10): 2866-2878.

Luisier, F., T. Blu and M. Unser, 2007. A new SURE approach to image denoising: Interscale orthonormal wavelet thresholding. IEEE Trans. Image Process., 16: 593-606.

Lysaker, M., A. Lundervold and X. Tai, 2003. Noise removal using fourth-order partial differential equations with applications to medical magnetic resonance images in space and time. IEEE Trans. Image Process., 12(12): 1579-1590.

Mıhcak, M.K., I. Kozintsev, K. Ramchandran and P. Moulin, 1999. Low complexity image denoising based on statistical modeling of wavelet coefficient. IEEE Signal Process. Lett., 6(12): 300-303.

Muresan, D.D. and T.W. Parks, 2003. Adaptive principal components and image denoising. Proceeding of International Conference on Image Processing, September 14-17, 1: I101-I104.

Pizurica, A., W. Philips, I. Lamachieu and M. Acheroy, 2002. A joint inter-and intra-scale statistical model for Bayesian wavelet based image denoising. IEEE Trans. Image Process., 11(5): 545-557.

Pizurica, A. and W. Philips, 2006. Estimating the probability of the presence of a signal of interest in multiresolution single and multiband image denoising. IEEE Trans. Image Process., 15(3): 654-665.

Rajan, J., K. Kannan and M.R. Kaimal, 2008. An improved hybrid model for molecular image denoising. J. Mathemat. Imag. Vision, 31: 73-79.

Rao, M., G. Venu and S. Vathsal, 2009. Local adaptive bivariate shrinkage function for medicalimage denoising. Int. J. Electr. Eng., 1(1): 59-65.

Rudin, L., S. Osher and E. Fatemi, 1992. Nonlinear total variation based noise removal algorithms. Phys. D, 60: 259-268.

Selesnick, I., 2009. A Derivation of the Soft-Thresholding Function. Polytechnic Institute of New York University.

Starck, J.L., E.J. Candes and D.L. Donoho, 2002. The curvelet transform for image denoising. IEEE Trans. Image Process., 11(6): 670-668.

Sendur, L. and I.W. Selesnick, 2002. Bivariate shrinkage functions for wavelet-based denoising exploiting interscale dependency. IEEE Trans. Signal Process., 50(11): 2744-2756.

Sendur, L. and I.W. Selesnick, 2002. Bivariate shrinkage with local variance estimation. IEEE Signal Process Lett., 9(12): 438-441

Tomasi, C. and R. Manduchi, 1998. Bilateral filtering for gray and colour images. The proceedings of IEEE International Conference on Computer Vision, Bombay, India, pp: 839-846.

You, Y. and M. Kaveh, 2000. Fourth-order partial differential equations for noise removal. IEEE Trans. Image Process., 9(10): 1723-1730.

Zhang, L., Z. Lei, M. Xuanqin and Z. David, 2011. FSIM: A feature similarity index for image quality assessment. IEEE Trans. Image Process., 20(8): 2378-2386.

Zhang, L., D. Weisheng, Z. David and S. Guangming, 2010. Two stage image denoising by principal component analysis with local pixel grouping. Pattern Recogn. Lett., 43: 1531-1549.